Scott Bair
Research Engineer.

W. O. Winer
Professor.

School of Mechanical Engineering, Georgia Institute of Technology, Atlanta, Ga. 30332

A Rheological Model for Elastohydrodynamic Contacts Based on Primary Laboratory Data

A shear rheological model based on primary laboratory data is proposed for concentrated contact lubrication. The model is a Maxwell model modified with a limiting shear stress. Three material properties are required: Low shear stress viscosity, limiting elastic shear modulus, and the limiting shear stress the material can withstand. All three are functions of temperature and pressure. In applying the model to EHD contacts the predicted response possesses the characteristics expected from several experiments reported in the literature and, in one specific case where direct comparison could be made, good numerical agreement is shown.

Introduction

The shear rheological response of lubricants in highly loaded contacts has been a vexing problem confronting the community for many years and has been the subject of much research and speculation. The environmental conditions to which the lubricant is subjected are apparently unique and very severe. It is essentially impossible to reproduce those conditions in primary laboratory measurements and consequently to date, concentrated contact traction has not been predictable from primary laboratory measurements. It is the purpose of this paper to present a simple rheological model of lubricant behavior in concentrated contacts, the necessary primary physical data, and to show how it can be used to predict EHD traction.

Johnson and Roberts [1] discuss the difficulty of distinguishing between different models from EHD data. This is particularly true in the low slide-roll ratio portion of the traction curve where small stains occur which could be either a viscous or elastic solid response. However, in their novel EHD experiments with controlled amounts of side slip and/or spin they convincingly demonstrate a viscous-solid transition and the inapplicability of the compressional visco-elasticity model.

Many different rheological models have been proposed but, apparently without exception, to predict contact behavior requires measurement of contact behavior and an adjustment of curve fitting material parameters. The discovery of the underlying physical properties seems to have escaped us to date. To be useful and readily accepted the primary physical properties and model employed must not only predict behavior accurately and distinguish between materials, but it must also be readily comprehended by those who must use the model. We believe that the model proposed in this paper meets these requirements. The model is likely to be considered suspect because of its simplicity or because with some modification it is a variation of other models proposed. It must be recognized that all the property data used to develop and apply the model are primary laboratory measurements independent of any EHD experiment.

Review of Observations

As we reported previously [2] the temperature at which liquid-solid transition occurs for low rate processes increases with pressure enough to insure solidlike behavior in many EHD contacts with many common materials. In that previous paper the transition was referred to as the glass-transition which is correct but misleading in that these materials have a low yield shear stress and are very ductile under pressure compared to that behavior which is normally associated with glasses. Therefore we will now refer to it as the solid-liquid transition. The rate of environmental change in an EHD contact is greater than that in the dilatometry experiment. This rate increase will shift the liquid-solid transition to increase the pressure-temperature region associated with the solidlike behavior. Therefore the dilatometry based transition measurements can be viewed as a bound on the lubricant behavior.

Johnson and Roberts [1] report liquid-solid transitions in an EHD contact based on traction measurements under well controlled and novel kinematics. They observed transitions by varying pressure at constant temperature and by varying temperature at constant pressure. The lubricant employed was not identical to any of those reported in [2] but in [2] we showed that several mineral oil based ma-

Contributed by the Lubrication Division of the American Society of Mechanical Engineers and presented at the ASME-ASLE Joint Lubrication Conference, Minneapolis, Minn., October 24-26, 1978. Manuscript received by the Lubrication Division, April 15, 1978, revised manuscript received June 15, 1978. Paper No. 78-Lub-9.

terials had very similar transition characteristics. The Johnson and Roberts [1] material was similar to but a higher viscosity than our naphthenic mineral oil (N1). The dilametry transition data for our mineral oils is shown in Figure 1 along with the EHD based transition points of Johnson and Roberts [1] and Johnson and Cameron [13]. The agreement between the two different kinds of measurements lends credibility to the relevance of the dilatometry data to EHD applications.

Fig. 2 is a heuristic diagram indicating how this solid-liquid transition might influence EHD contacts for three representative lubricants. If the transition occurs in the Hertzian zone it would be expected to influence the contact traction while if it occurs in the inlet zone it would also affect the film thickness. As seen in Fig. 2, 5P4E is the most likely to experience the transition not only in the Hertzian zone but also the inlet zone at least at moderate temperatures. The transition of the mineral oil will only occur in the inlet zone for low temperature applications and in the Hertzian zone for higher pressure applications. The synthetic paraffin mineral oil (XRM 177) is far less likely to experience the transition in the inlet zone and it will occur in the Hertzian zone only for very high pressure contacts.

The above leads one to ask about the shear rheological properties in the solid region and near the transition zone for the magnitude of strain expected in an EHD contact. In the liquid region the shear rheological behavior would be expected to be classical viscous behavior with possible viscoelastic phenomena at high rates of change of stress. Well into the solid region elastic behavior for small strains would be expected with some limit to the elastic stress and strain that the material can withstand before yielding. Near the transition curve the behavior would be expected to be some complex combination of viscous, elastic, and plastic behavior. In determining the shear rheological behavior of lubricants we must determine what is meant by "well into," "near," "small strain," and "high rates of change of shear stress," relative to the lubricants employed and concentrated contact kinematics and dynamics.

In a companion paper [3] we have reported shear rheological measurements on three lubricants[1] in the solid region and near the transition curve. The materials exhibited classical elastic behavior for small strains, limiting yield shear stress for large strains and large stresses, and viscous behavior for large strain small stress. The latter case agrees well with ordinary falling body viscosity data. In this paper we take that data and show how the viscous, elastic, and plastic characteristics of the materials can be unified into a straightforward Maxwell model with non-linear viscosity. The primary rheological properties will then be employed in the model to predict EHD traction.

The elastic-plastic behavior of 5P4E is shown in Fig. 3 which is a typical shear stress-shear strain curve taken in the solidlike region of behavior [3]. The limiting elastic shear modulus, $G_\infty(t, p)$ (Fig. 4) measured on 5P4E at 275 MPa is 1.2 GPa and agrees with that measured ultrasonically by Barlow [4] at the same pressure and a much higher rate. The recoverable elastic strain is only about 0.03 which is small compared to that occurring in most EHD contacts at moderate to high slide-roll ratios. For larger strains the material exhibited a yield shear stress which reached a maximum value as the shear rate was increased. The limiting shear stress, τ_L, and the limiting shear modulus, G_∞, are related through the maximum recoverable elastic shear strain, γ_{RE}, by the approximate relation

$$\tau_L = G_\infty \gamma_{RE}. \tag{1}$$

Therefore the limiting yield shear stress is about a factor of thirty less than the elastic shear modulus. Additional data for the limiting shear stress as a function of temperature and pressure is given for the three materials in [3].

Large strain visco-plastic behavior is shown in Figure 5 from two types of measurements; low shear rate falling body viscosity and high stress viscosity measurements [3]. The agreement between the measurements is apparent and the decrease in apparent viscosity along a line of constant shear stress is also clear. This is inherent material behavior and not viscous heating which would cause the inflexion of the apparent viscosity curve to occur at the line of constant energy input rate per unit volume (shear stress times shear rate). Figure 5a is for 5P4E and 5b for Santotrac 50.

The above two types of viscosity measurement (Fig. 5) and the yield shear stress data such as that in Fig. 3 are shown in Figs. 6(*a*), (*b*) for 5P4E at 40C and 60C, respectively, and in Fig. 7 for Santotrac 50 at 20C. In these figures for the large strain behavior, the data in the upper left hand group was obtained in a high stress low rate device

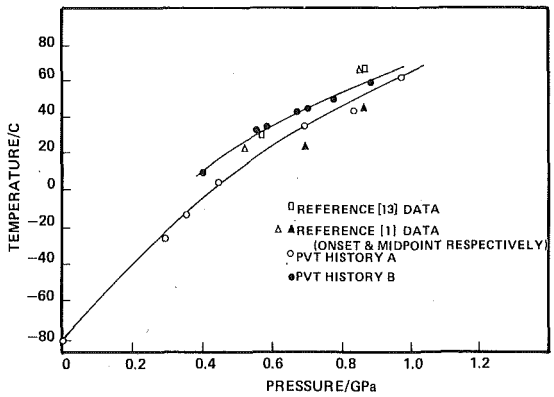

Fig. 1 Comparison of glass transition of N1 by various PVT methods and liquid-solid EHD transition data of Johnson, et al. [1, 13]

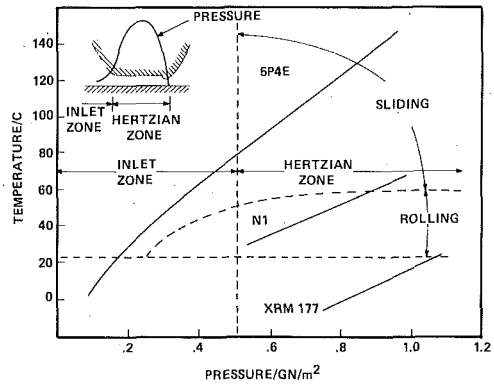

Fig. 2 Heuristic estimates of the relationship between conditions in an EHD contact and glass-liquid transition diagram of some lubricants (lubricant supply temperature about 20C)

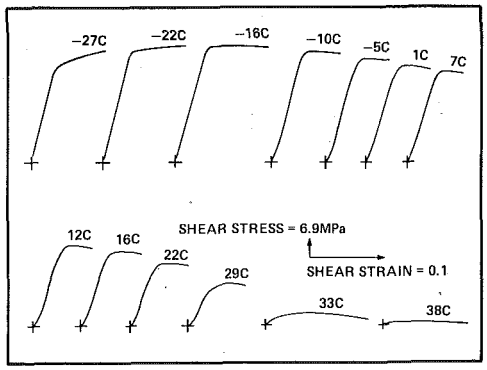

Fig. 3 Recorder plot of shear stress versus shear strain for polyphenyl ether (5P4E) at 0.275 GPa (40 kpsi) and indicated temperatures

[1] Polyphenyl ether (5P4E), naphthenic mineral oil (N1), and cycloaliphatic synthetic hydrocarbon (Santotrac 50).

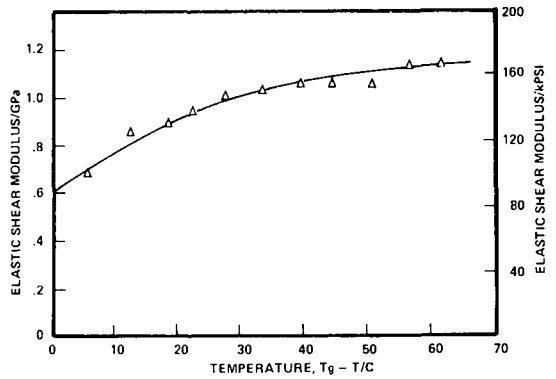

Fig. 4 Elastic shear modulus of polyphenyl ether (5P4E) at 0.275 GPa (40 kpsi) in amorphous glassy region

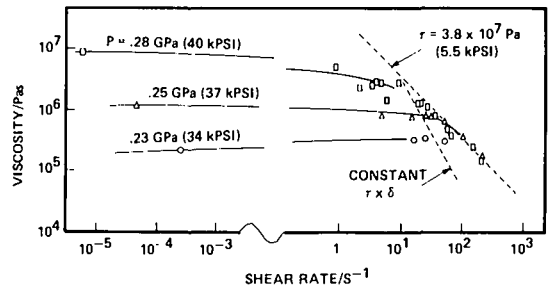

Fig. 5(*a*) Viscosity of 5P4E versus shear rate showing the limiting shear stress at 40C

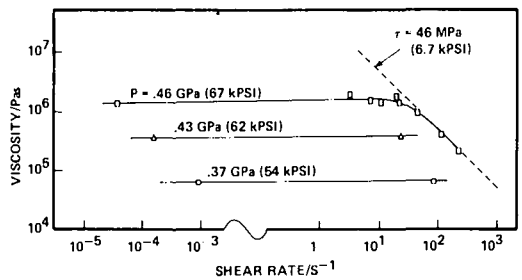

Fig. 5(*b*) Viscosity of Santotrac-50 versus shear rate showing limiting shear stress at 20C

[3], that in the upper right hand group was obtained in a high stress-high rate device [3], and that at the bottom was obtained in a standard falling body viscometer which is a very low constant stress device. On this type of plot Newtonian viscous behavior is represented by a straight line with slope of one. Therefore it is seen how the viscometer and high stress data complement each other. The limiting shear stress increases somewhat with pressure but the effect is small on the scale of these figures.

Fig. 8 also shows how the viscosity obtained from the high stress data (upper left-hand part of Fig. 6(*b*)) and that from the high stress viscometer (upper right hand part of Fig. 6(*b*)) are consistent with the low shear stress falling body viscosity-pressure data for 5P4E at 60C. Also shown in Fig. 8 are the apparent viscosities predicted at constant shear rate by the model discussed subsequently in the paper. If the viscosity was measured as a function of pressure at the constant temperature and the steady shear rate given, it would follow the usual curve up to the point shown and then go off nearly horizontal. The lower the shear rate, the higher the point of departure. The slope of the curve after it departs from the low shear rate curve is the rate of change of the limiting shear stress with pressure.

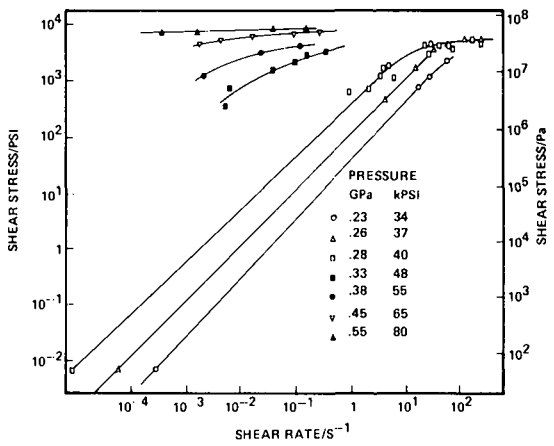

Fig. 6(*a*) Shear stress-shear strain rate for 5P4E at 40C and indicated pressure (three different methods-see text)

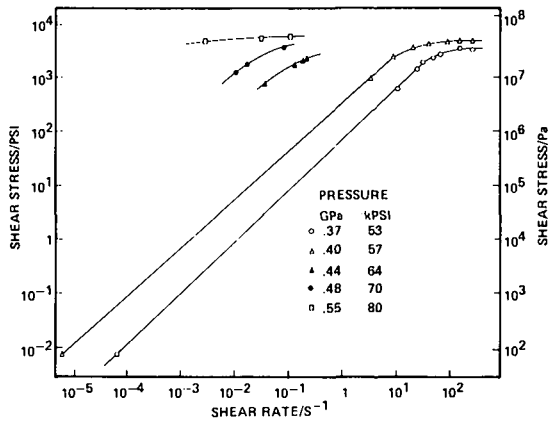

Fig. 6(*b*) Shear stress-shear strain rate for 5P4E at 60C and indicated pressure (three different methods-see text)

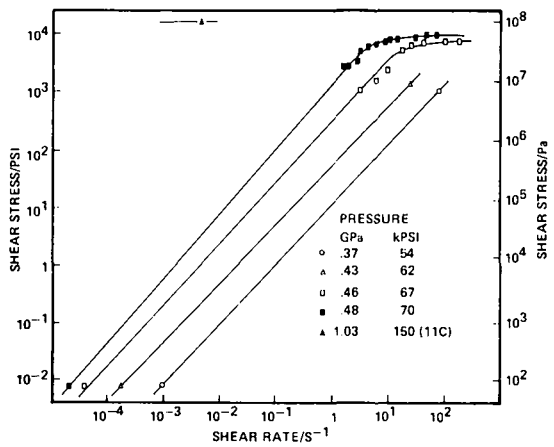

Fig. 7 Shear stress-shear strain rate for Santotrac 50 at 20C and indicated pressures (three different methods-see text)

The pattern of the data in Figs. 5 thru 7 suggests a straightforward shifting of the data by nondimensionalization. The shear stress can be non-dimensionalized by dividing by the maximum or limiting yield shear stress, $\tau_L(p, T)$, and the shear rate can be nondimensionalized by multiplying by the low shear stress viscosity, $\mu_0(p, T)$, and dividing by the limiting yield shear stress, $\tau_L(p, T)$. The non-dimensionalized data from both Figs. 6 and 7 are presented in Fig. 9.

Several physical interpretations can be given to these dimensionless

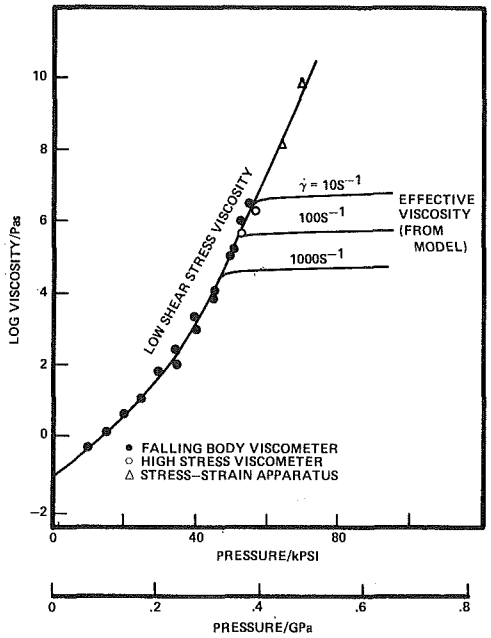

Fig. 8 Viscosity pressure isotherm (60C) for 5P4E by indicated methods of measurement. Lines of constant shear rate predicted form model

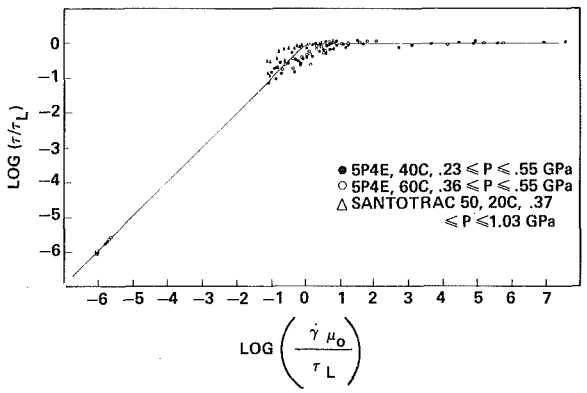

Fig. 9 Dimensionless shear stress versus dimensionless shear rate for indicated data

parameters. The dimensionless shear stress, $\hat{\tau} = \tau(p, T)/\tau_L(p, T)$ (ordinate) is the ratio of the actual shear stress to the limiting yield shear stress the material can withstand at the given temperature and pressure. The dimensionless shear rate, $\dot{\gamma} = \dot{\gamma}\mu_0(p, T)/\tau_L(p, T)$ (abscissa), can be thought of as; (*a*) the ratio of the shear stress that would prevail if Newtonian viscous behavior was followed, to the limiting yield shear stress; (*b*) as the actual shear rate times a visco-plastic flow relaxation time t_p, where $t_p \equiv \mu_0(p, T)/\tau_L(p, T)$, or (*c*) the dimensionless shear rate might also be thought of as a Deborah number of visco-plastic transition because $\dot{\gamma} = 1$ is the middle of the transition from Newtonian viscous behavior ($\dot{\gamma} < 1$) to limiting shear stress plastic flow behavior ($\dot{\gamma} > 1$). Yet another interpretation might be that the dimensionless shear rate is the time derivative of the shear strain scaled to the recoverable elastic strain with respect to a dimensionless time obtained by scaling time with the elastic relaxation time.

The visco-plastic flow relaxation time is related to the viscoelastic relaxation, $t_e = \mu_0(p, T)/G_\infty(p, T)$, by the recoverable elastic shear strain γ_{RE}

$$t_p = \frac{\mu_0(p, T)}{\tau_L(p, T)} \cdot \frac{G_\infty(p, T)}{G_\infty(p, T)} = t_{\hat{e}} \frac{G_\infty(p, T)}{\tau_L(p, T)} = t_{\hat{e}} \frac{1}{\gamma_{RE}} \tag{2}$$

or

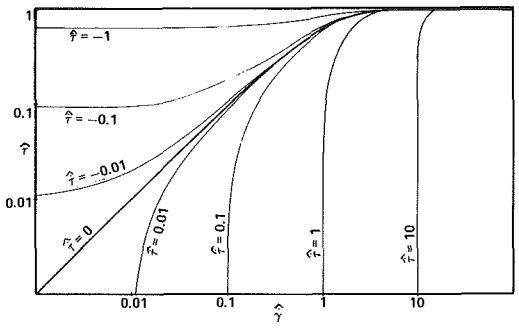

Fig. 10 Dimensionless shear stress-shear rate plot from model (equation (5)) for indicated values of dimensionless rate of shear stress application

$$\gamma_{RE} = \frac{t_e}{t_p}.$$

As we have shown above, the recoverable elastic shear strain is about 0.03. Therefore the visco-plastic relaxation time is about 30 times longer than the visco-elastic relaxation time.

Proposed Flow Model

The flow data shown in Figs. 5 thru 7 and nondimensionalized as described above are shown in Fig. 9. It shows that this approach coordinates the measured data over a wide range of pressures and temperatures as well as over many orders of magnitude of shear stress and shear strain rate for both materials. The visco-plastic data can be described reasonably well with a single natural log function. The relationship proposed for the large strain flow behavior is

$$\hat{\dot{\gamma}} = -\ln(1 - \hat{\tau}) \tag{3}$$

and is shown as the solid curve in Fig. 9. This can be viewed as a nonlinear viscous flow equation.

If this relation is introduced as the viscous part of the usual Maxwell visco-elastic model, we get a modified Maxwell model of

$$\hat{\dot{\gamma}} = \hat{\dot{\gamma}}_e + \hat{\dot{\gamma}}_v \tag{4}$$

or

$$\hat{\dot{\gamma}} = \dot{\tau} - \ln(1 - \hat{\tau}) \tag{5}$$

where $\hat{\dot{\gamma}}$ and $\hat{\tau}$ are described as above and

$$\hat{\dot{\tau}} = \frac{\mu_0}{\tau_L G_\infty} \frac{d\tau}{dt} = t_e \frac{d\left(\frac{\tau}{\tau_L}\right)}{dt} = \frac{d\left(\frac{\tau}{\tau_L}\right)}{d\left(\frac{t}{t_e}\right)} = \frac{d\hat{\tau}}{d\hat{t}} \tag{6}$$

Equation (5) is the dimensionless form of the proposed shear rheological equation and is shown in Fig. 10, where all three kinds of behavior are seen.

The dimensionless form of the proposed modified Maxwell Model, equation (5), obscures the familiary primary physical data required to implement it. Equation (7) is a dimensional form of the model

$$\dot{\gamma} = \frac{1}{G_\infty} \frac{d\tau}{dt} - \frac{\tau_L}{\mu_0} \ln\left(1 - \frac{\tau}{\tau_L}\right) \tag{7}$$

From equation (7) it is seen that the three primary physical properties required to use the model are low shear stress viscosity, μ_0, the limiting elastic shear modulus, G_∞, and the limiting yield shear stress, τ_L, all as functions of temperature and pressure. By the relationships mentioned previously either or both of the last two (G_∞ and τ_L) could be replaced by one or two of the following three properties; viscoelastic relaxation time (t_e), visco-plastic relaxation time (t_p), or recoverable elastic strain (γ_{RE}). The three primary properties (μ_0, G_∞, τ_L) are probably the most logical to pursue.

Several techniques have been available for some time to measure μ_0 and G_∞ and the measurement of τ_L is relatively straightforward

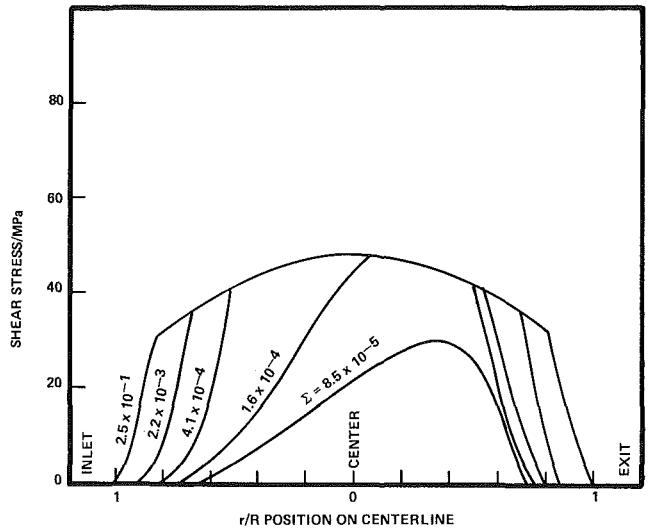

Fig. 11 Predicted shear stress distribution in point contact for Santotrac 50 at 20C, 0.5 GPa Hertz pressure, 0.22 m/s rolling speed and indicated slide roll ratios based on equation (5) and measured data

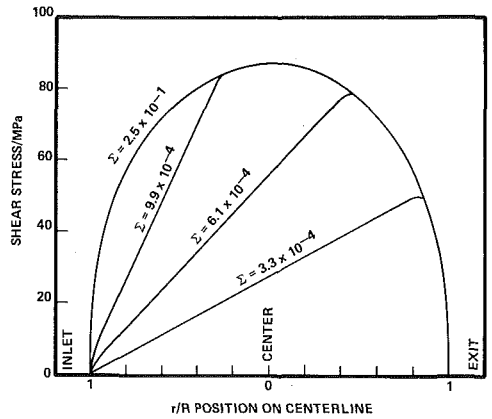

Fig. 12 Predicted shear stress distribution in point contact for 5P4E at 40C, 1.0 GPa. Hertz pressure, 0.22 m/s rolling speed and indicated slide roll ratios based on equation (5) and measured data

as described in our companion paper [3]. We have the capability of measuring all three of these properties over a range of pressures and temperatures and have presented the data elsewhere (for μ_0 cf. [5–8], for τ_L and G_∞ cf. [3, 5]). Several other sources of pressure viscosity and elastic shear modulus are available in the literature (the work of Lamb, et al. [cf. 4, 9], Harrison [10], and Dill and Litovitz, et al. [cf. 11] to mention only a few).

Application of the Model to EHD Traction Prediction

We have employed the above model to predict shear stress and traction in EHD point contacts. The properties used are the three primary material properties mentioned above and measured in our laboratory. The contact was divided nonuniformly into a grid of 20 segments on a cord in the direction of motion and 20 such strips across the contact perpendicular to the direction of motion to permit pressure and material property variation in the contact. The following assumptions were employed; the film thickness and material temperatures were assumed uniform throughout the contact, the pressure distribution was Hertzian, no twist or side slip was present, the viscosity was an exponential function of pressure, the elastic shear modulus was constant, and the elastic surface compliance was proportional to the contact traction as developed by Kalker [12] and reported in Johnson and Roberts [1], and inlet zone effects were neglected. Several of these assumptions can be called into question and should be refined in subsequent development particularly those concerned with the temperature distribution and failure to include the inlet zone influence. However, they are acceptable for a first test of the model and seem to be justified as the results will show.

Although we know the assumption of constant film temperature is not true, the analysis is done for slide-roll ratios of less than one tenth. From other work in this laboratory [14, 15] under conditions to those used in this analysis we know the maximum surface temperature rise is usually less than 5C above the bulk temperature in this range. Although we have not measured lubricant temperatures at these low slide-roll ratios, work in sliding contacts would indicate they are probably less than 5 to 10C above the surface temperature.

With the above assumptions a program was written to calculate the local shear stress at each point in the grid by using a Bisection Method on the model equation with starting shear stresses of zero and 0.999 τ_L. If the Bisection Method does not find a solution as the trial shear stress reaches 0.999 τ, the solution is assumed to be τ_L. To obtain the time derivative term, upstream grid positions plus a convective derivative are employed for a given grid point. The average shear stress in the contact is obtained by integration over the area and the traction coefficient is the ratio of the average shear stress divided by the average pressure.

Fig. 11 is a plot of the shear stress along the centerline in the direction of motion (from left to right) at various slide-roll ratios for Santotrac 50 at 20C, a Hertz pressure of 0.5 GPa, and a rolling velocity of 0.22 m/s. The film thickness used was 0.2 μm. As seen at the lowest slide-roll ratio the limiting shear stress is not reached, but at a slide-roll ratio of about 10^{-4} the limiting stress value is reached somewhat passed the center of the contact. As the slide-roll ratio is further increased the region where the limiting shear stress occurs grows as an area spreading outward to cover the entire contact. As seen from the traction coefficient data tabulation this growth of the limiting shear stress region is occurring while the traction is increasing to its maximum value. The variation of properties over the contact is important. In the cases shown in Figure 11 the shear stress is predominantely viscous except where the limiting value is reached. This is primarily because of the pressure selected for the example (p_H = 0.5 GPa). At a higher pressure or lower temperature this material would also show elasto-plastic behavior as the 5P4E does in Fig. 12.

Fig. 12 shows the shear stress distribution for a similar calculation with 5P4E. In this case no viscous behavior is seen, only elastic and limiting shear stress plastic behavior. The area of limiting shear stress starts at the exit region and grows forward as the slide-roll ratio increases from about 10^{-4} to about 10^{-2} when the limiting shear stress occurs over the entire contact.

In the above cases we saw examples of visco-plastic and elasto-plastic behavior on shear stress distribution. It is instructive to take one of these materials and look at the predicted traction curve for various limiting cases of the model compared to the complete model. The viscoelastic case occurs by requiring the limiting shear stress to be very large compared to any shear stress value expected in the contact. Equation (7) of the model then becomes the classical Maxwell model of

$$\dot{\gamma} = \frac{1}{G_\infty}\frac{d\tau}{dt} + \frac{\tau}{\mu_0}. \tag{7a}$$

The limiting case of visco-plastic results from specifying a very large value for G_∞ so the model becomes the nonlinear viscous from of

$$\dot{\gamma} = -\frac{\tau_L}{\mu_0}\ln\left(1 - \frac{\tau}{\tau_L}\right) \tag{7b}$$

The third possibility of elastic-plastic behavior is obtained by letting the viscosity take on a very large value in which case all the strain at low stress occurs in the elastic term and at large stress the limiting stress controls. This special case model equation looks just like equation (7). Any change in appearance would lose an essential feature. The traction slide-roll ratio curve predicted by these three special cases and the complete model are shown in Figure 13 for 5P4E at the conditions indicated. For this material and the conditions used, the essential features are the elastic behavior at low slide-roll ratio and plastic behavior at higher slide-roll ratio. The transition slide-roll

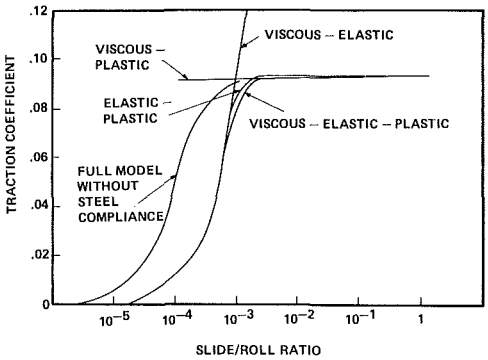

Fig. 13 Traction coefficient versus slide-roll ratio for indicated special cases of model (equation (5)) for 5P4E, 40C, 1.0 GPa Hertz pressure, and rolling velocity of 0.22 m/s

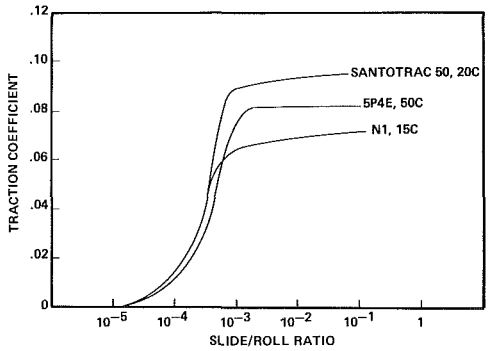

Fig. 15 Predicted traction coefficient (Model equation (5) and measured properties) versus slide-roll ratio for indicated lubricants and temperatures at 1.0 GPa Hertz pressure and 0.22 m/s rolling speed

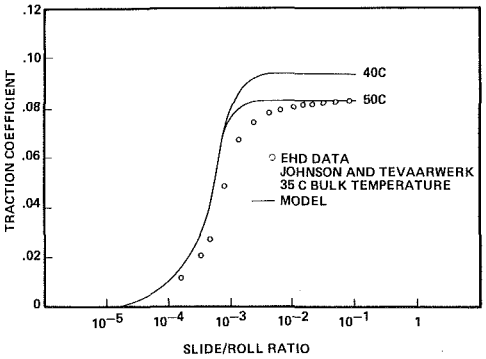

Fig. 14 Traction coefficient versus slide-roll for 5P4E, 1.0 GPa Hertz pressure, rolling velocity of 0.22 m/s and indicated temperature. Comparison of model prediction (equation (5)) and measurements of Johnson and Tevaarwerk [20]

ratio is only 10^{-3}, however, which is a small value and attained only in the better, well controlled traction devices. Neither the visco-elastic nor visco-plastic models are appropriate over the entire range. The influence of surface compliance is to shift the slide-roll ratio to increasing values. Surface compliance is included in all the calculations presented in this paper. If it were not included the curve so marked in Fig. 13 would be predicted during the rise in traction coefficient for the full model. Once the peak traction is reached surface compliance effects can no longer be seen.

Comparison With Measured EHD Traction

The necessary test for a proposed model is the comparison of predicted values with measured values in an EHD traction device. As seen from the above predictions the most important parts of the curve to check are the low slide-roll ratio range and the maximum values. Our own traction device at this time does not have adequate control in crucial low slide-roll ratio range and therefore we must rely on the data in the literature of which there is a great deal (i.e., Cheng and Trachman [16], Dyson [17], Smith, et al. [18], Hirst, et al. [19] and Johnson, et al. [1, 13, 20]). Any choice is complicated by the need to know the magnitude and precision of both operating conditions and the data as well as the relationship between the lubricant used and the material we used to determine the primary physical properties for the model. We therefore choose for the first comparison the data of Johnson and Tevaarwerk [20] on 5P4E. The material is well defined and the major possible variations would be lot-to-lot variation and contamination of either sample both of which we think were small.

Fig. 14 is a plot of traction coefficient against slide-roll ratio for 5P4E at 1 GPa Hertz pressure and rolling velocity of 0.22 m/s. The data points are those reported by Johnson and Tevaarwerk [20] for a bulk temperature of 40C. The two solid curves are predicted by the model using the film thickness to Hertz diameter in [120] and average film temperatures of 40C and 50C. Both curves agree with the data when the basis of the model is considered and the difficulties encountered in attempting such a prediction in the past. The 50C curve not only agrees with the data better than the 40C curve but also is a more reasonable assumption for the film temperature if the bulk temperature is 40C. We have shown elsewhere [14, 15] that for these low slide-roll ratios, pressures and velocities the surface temperature will increase 5 to 8C above the bulk and the film must be somewhat higher. The agreement shown in Figure 14 indicates that the proposed approach to EHD traction is promising and deserving of further development.

Fig. 15 shows the predicted traction curves for the three materials for which we currently have a sufficient amount of primary data. Although the pressures and kinematics are the same for the three materials, the temperatures are different because of the ranges of material properties available. In the cases of N1 and Santotrac 50 a noticeable portion of the traction is the result of viscous action even at the higher slide-roll ratio. This accounts for the continued increase in traction for slide-roll ratio greater than 10^{-3}. The plastic flow zone is still spreading with increasing slide-roll ratio as shown in Fig. 11. The 5P4E, however, for slide-roll ratios greater than 10^{-3} has the entire area covered by the plastic flow zone (Fig. 12) and therefore only thermal effects or changing pressures will change the traction in that range. Hence the zero slope to the traction curve. Caution must be exercised in generalizing about the relative maximum traction shown for these three materials because the limiting shear stress dependence on temperature and pressure for the three materials is different.

If we consider a material and set of conditions which produce primarily visco-plastic flow (such as shown in Fig. 11), and consider an EHD experiment with increasing load and fixed kinematics, we could observe an effective viscosity of the material. This is essentially one of the experiments of Johnson and Cameron [13]. In our model (equation (5)) this would be comparable to considering constant shear rate, no elastic effects, and increasing pressure. The ratio of shear stress to shear rate is the apparent viscosity. The results of this calculation are shown along with the low stress pressure viscosity for several constant shear rates in Fig. 8. The lower the shear rate the higher the viscosity where the apparent viscosity begins to diverge from the low stress viscosity curve. The slope of the curve after the divergence is the limiting shear stress dependence on pressure.

Conclusion

We believe we have found and, at least partially, substantiated a simple visco-elasto-plastic material shear rheological model employing measured primary laboratory data which predicts measured EHD traction under typical operating conditions. The model incorporates the three classical forms of material shear behavior, Newtonian viscous, Hookean elastic and plastic yield. The identification of the controlling material properties (μ_0, G_∞, τ_L) will aid designers and material synthesizers because of the small quantities of material required to determine the properties [3]. The limiting yield shear stress

determines the maximum traction which can be transmitted in an EHD contact. The variation of that property with temperature and pressure will be important to contact traction behavior.

The results presented show how the transition to plastic yield influence the traction as the yielded region in the contact spreads. It was seen that the transition spreads toward the inlet region and therefore one would expect that as the transition moves into the inlet zone it may also influence the film thickness. The effect would most likely be to decrease the film thickness compared to the values predicted for the usual viscous material model. This has been studied by Wilson and Aggrawal [21] for metalworking and needs to be explored for elastohydrodynamic lubrication.

Acknowledgment

The authors wish to acknowledge the support of NASA-Lewis Laboratories through a Grant (NSG-3106) and to express their appreciation for the continual interest and encouragement of Mr. W. J. Anderson, Branch chief, and the contract monitors, Drs. William Jones and L. D. Wedeven.

References

1 Johnson, K. L., and Roberts, A. D., "Observations of Viscoelastic Behavior of an Elastohydrodynamic Lubricant Film," *Proceedings of the Royal Society of London,* Vol. 337A, 1974, pp. 217–242.

2 Alsaad, M., Bair, S., Sanborn, D. M., and Winer, W. O., "Glass Transitions in Lubricants: Its Relation to EHD Lubrication," ASME JOURNAL OF LUBRICATION TECHNOLOGY, Vol. 100, July 1978, pp. 404–417.

3 Bair, S., and Winer, W. O., "Shear Strength Measurements of Lubricants at High Pressure," published in this issue, pp. 251–257.

4 Barlow, A. J., Erginsav, A., andLamb, J., "Viscoelastic Relaxation in Liquid Mixtures," *Proc. Roy. Soc. of London,* 309A, 1969, pp. 473–496.

5 Sanborn, D. M., and Winer, W. O., "Investigation of Lubricant Rheology as Applied to Elastohydrodynamic Lubrication," NASA Grant No. NSG-3106, Report, Nov. 1977.

6 Jones, W. R., Johnson, R. L., Sanborn, D. M., and Winer, W. O., "Viscosity-Pressure Measurements for Several Lubricants to 5.5×10^8 N/m^2 (8×10^4 psi) and 149C (3]]F), *Trans. ASLE,* Vol. 18, No. 4, 1975, pp. 249–262.

7 Novak, J., and Winer, W. O., "Some Measurements of High Pressure Lubricant Rheology," ASME JOURNAL OF LUBRICATION TECHNOLOGY, Vol. 90, No. 3, 1968, pp. 580–591.

8 Jakobsen, J., Sanborn, D. M., and Winer, W. O., "Pressure Viscosity Characteristics of a Series of Siloxanes", ASME JOURNAL OF LUBRICATION TECHNOLOGY, Vol. 96, 1974, pp. 410–417.

9 Lamb, J., "Physical Properties of Fluid Lubricants: Rheological and Viscoelastic Behavior," *Proc. Inst. Mech. Engrs.,* Vol. 182, Part 34, 1967–1968, pp. 293-310.

10 Harrison, G., *The Dynamic Properties of Supercooled Liquids,* Academic Press, 1976.

11 Dill, J. F., Drake, P. W., and Litovitz, T. A., "The Study of Viscoelastic Properties of Lubricants Using High Pressure Optical Techniquies," *Trans ASLE,* Vol. 18, No. 3, 1975, p. 202.

12 Kalker, J. J., *Proc. K. Ned. Akad. Wet.,* Vol. B67, p. 135.

13 Johnson, K. L., and Cameron, R., "Shear Behaviour of Elastohydrodynamics Oil Films at High Rolling Contact Pressures," *Proc. Inst. Mech. Engrs.,* Vol. 182, Part 1, 1967-1968, pp. 307-319.

14 Nagaraj, H. S., Sanborn, D. M., and Winer, W. O., "Surface Temperature Measurements in Rolling and Sliding EHD Contacts," ASLE Paper no. 78-AM-2B-2 (to be published in *ASLE Trans. 1979*).

15 Nagaraj, H. S., Sanborn, D. M., and Winer, W. O., "Direct Surface Temperature Measurements by Infrared Radiation in EHD, and the Correlation of the Blok Flash Temperature Theory," *Wear,* Vol. 49, 1978, pp. 43–59.

16 Trachman, E. G., and Cheng, H. S., "Traction in Elastohydrodynamic Line Contacts for Two Synthesized Hydrocarbon Fluids," ASLE Paper No. 73LC-4A-1, (1973).

17 Dyson, A., "Frictional Traction and Lubricant Rheology in Elastohydrodynamic Lubrication," *Philosophical Trans. Roy. Soc. of London,* Vol. 266A, 1970, p. 1.

18 Smith, R. L., Walowit, J. A., and McGrew, J. M., "Elastohydrodynamic Traction Characteristics of 5P4E Polyphenyl Ether," ASME JOURNAL OF LUBRICATION TECHNOLOGY, Vol. 95, 1973, pp. 353–362.

19 Adams, D. R., and Hirst, W., "Frictional Traction in Elastohydrodynamic Lubrication," *Proc. Roy. Soc. of London,* 332A, 1973, pp. 505–525.

20 Johnson, K. L., and Tevaarwerk, J. L., "Shear Behavior of Elastohydrodynamic Oil Films," *Proc. Roy. Soc. of London,* Vol. 356A, 1977, pp. 215–236.

21 Wilson, W. R. D., and Aggrawal, B. B., "A Plastohydrodynamic Inlet Zone Analysis for a Visco-Plastic Lubricant," *Wear,* Vol. 47, 1978, pp. 119–132.